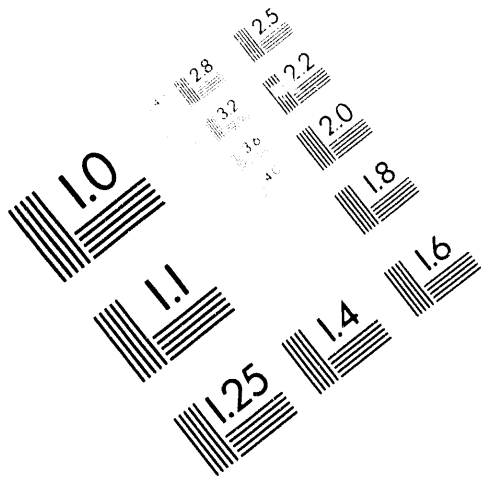

Association for Information and Image Management

1100 Wayne Avenue, Suite 1100
Silver Spring, Maryland 20910

301/587-8202

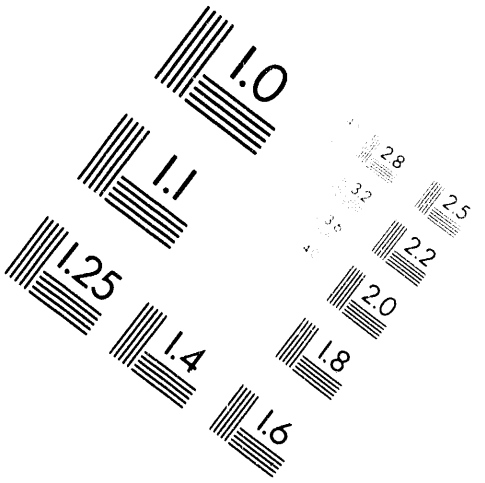

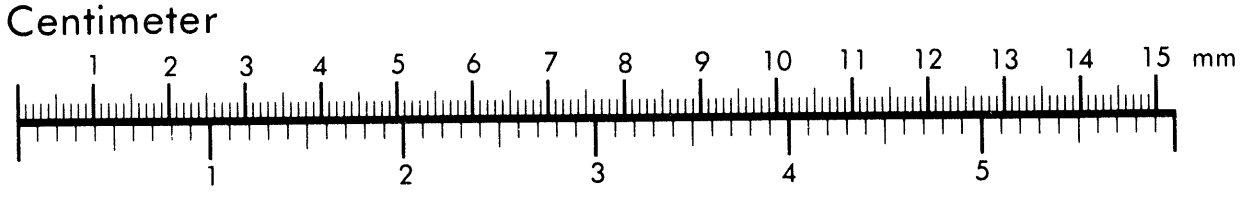

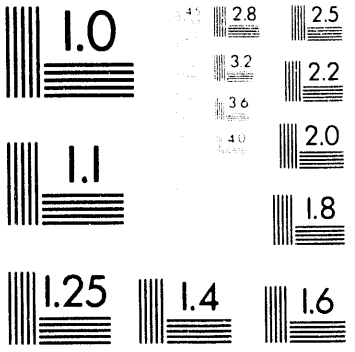

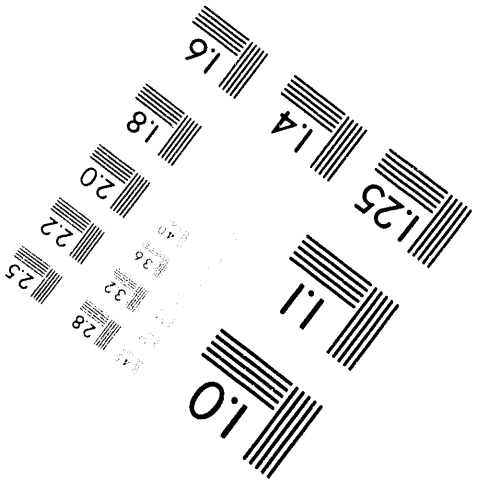

MANUFACTURED TO AIIM STANDARDS
BY APPLIED IMAGE, INC.

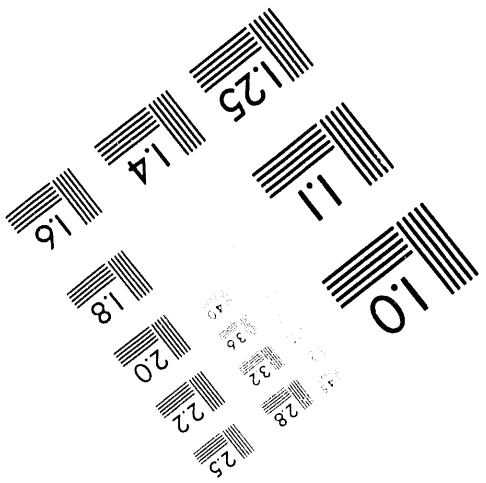

1 of 1

To be presented at the 10th International Heat Transfer Conference, Brighton, England, August 14-18, 1994.

MICROSCOPIC IMAGE PROCESSING SYSTEMS FOR MEASURING NONUNIFORM FILM THICKNESS PROFILES

A-H Liu, J. L. Plawsky, S. DasGupta and P. C. Wayner, Jr.

The Isermann Department of Chemical Engineering, Rensselaer Polytechnic Institute, Troy, New York 12180-3590

ABSTRACT

In very thin liquid films, transport processes are controlled by the temperature and the interfacial intermolecular force field which is a function of the film thickness profile and interfacial properties. The film thickness profile and interfacial properties can be measured most efficiently using a microscopic image processing system, IPS, to record the intensity pattern of the reflected light from the film. There are two types of IPS: an image analyzing interferometer (IAI) and/or an image scanning ellipsometer (ISE).

The ISE is a novel technique to measure the two dimensional thickness profile of a nonuniform, thin film, from 1 nm up to several μm, in a steady state as well as in a transient state. It is a full field imaging technique which can study every point on the surface simultaneously with high spatial resolution and thickness sensitivity, i.e., it can measure and map the 2-D film thickness profile. Using the ISE, the transient thickness profile of a draining thin liquid film was measured and modeled. The interfacial conditions were determined *in situ* by measuring the Hamaker constant. The ISE and IAI systems are compared.

1 INTRODUCTION

Transport processes in very thin liquid films are of generic importance to heat transfer technology. In these systems, the temperature and the interfacial intermolecular force fields control fluid flow and change-of-phase heat transfer. It is important to emphasize at this point that due to fluid mobility, the non uniform film shape is a function of the stress (pressure) field. This was discussed by Wayner [1991] and DasGupta et al. [1993] who used classical change-of-phase kinetics and interfacial concepts like the Kelvin-Clapeyron, Young-Dupré, and augmented Young-Laplace equations to evaluate and compare stress and thermal effects. Experimental confirmation of the use of the augmented Young-Laplace to model the stress field in thin liquid films was obtained using an image analyzing interferometer, IAI, to measure the film thickness profile. The importance of correctly modeling transport processes in ultra thin films was demonstrated recently in the following papers: Swanson & Peterson [1993]; Khrustlalev & Faghri [1993]; Wu & Peterson [1991]; Brown et al. [1993] and Xu & Carey [1990]. However, recent results also demonstrated that more powerful and convenient microscopic experimental techniques are needed to study thinner and smaller dynamic systems. In order to obtain more detail in the thinner region, a new experimental technique, image scanning *ellipsometry*, ISE, which uniquely combines ellipsometry, image processing, and a specific algorithm, has been developed and is described herein. Results obtained using both the ISE and IAI in the film thickness region $\delta < 5$ μm are discussed and compared.

If the bulk physical properties of the evaporating thin liquid film are known, the film thickness profile and interfacial conditions, measured experimentally, can be used with the temperature to calculate the heat transfer characteristics of the film. Therefore, one of the major experimental objectives of thin film heat transfer research is to determine the film thickness profile as a function of the experimentally varied evaporation rate and interfacial properties. In order to measure the thickness profile, the following equipment characteristics are required: (1) The instrument should be able to measure nonuniform films as well as uniform films from 1 nm up to several μm in thickness; (2) The instrument should be able to measure the thickness profile in the transient state as well as in the steady state; (3) The instrument should be able to measure every point on the liquid surface simultaneously instead of an average value over the measured surface. The other major experimental objective is the characterization of the interfacial conditions *in situ* which are needed to model thin film transport processes. This is accomplished by measuring the Hamaker constant of the liquid-solid system. All of the above objectives can be reached with the ISE.

Many different optical and non-optical techniques have been developed to measure film thickness profiles. However, none of these techniques had all the required characteristics mentioned above. The optical methods based on interferometry, in general, can measure non uniform films but cannot easily (because they depend on the intensity of the reflected light) measure film thicknesses under 1000 Å nor are they appropriate for uniform films. Image Analyzing Interferometry, IAI, is a new technique based on interferometry which was developed to measure non uniform film thickness profiles [DasGupta et al.,1993]. IAI not only has very good thickness sensitivity and lateral resolution but can

DISCLAIMER

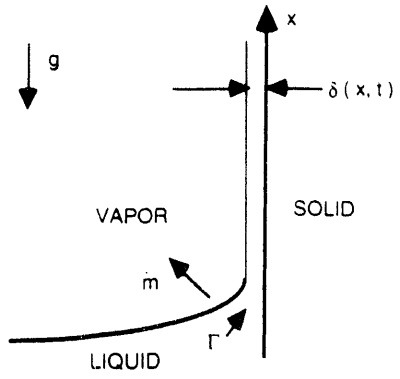

Figure 1. Vertical nonuniform film on solid substrate with fluid flow and and change-of-phase heat transfer.

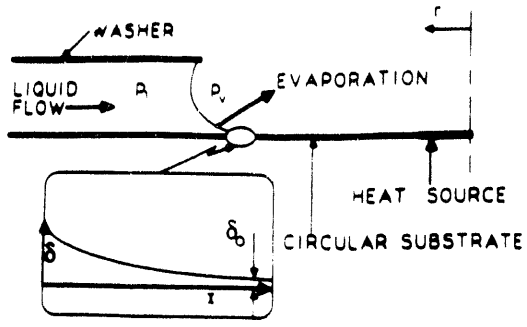

Figure 2. Steady state evaporating extended meniscus. The details in the figure are not to scale. The gap between the washer and the substrate was 0.5mm. DasGupta, et al. (1993).

also be used to study every point on a surface simultaneously by using image processing technology and a low-light-level CCD camera. However, one aspect that IAI is not well suited for is transient state studies: IAI uses a standard, time consuming, null ellipsometer, to extrapolate the measurement of the film thickness beyond the first interference minimum, $\delta < 1000$ Å. Herein, we discuss and compare the IAI with a modified form of ellipsometry, ISE, which obviates this disadvantage.

2. THIN FILM THEORY

Herein, we focus on single component curved thin films with negligible surface tension gradients. A mass balance for a thin film (e.g., the vertical non uniform film presented in Fig. 1 or the meniscus in Fig. 2) is

$$\rho_l \frac{\partial \delta}{\partial t} = -\frac{\partial \Gamma}{\partial x} - \dot{m} \qquad (1)$$

Both the mass flow rate, Γ, and the local interfacial mass flux, $\dot{m}$, are functions of the film thickness profile, $\delta(x,t)$. However, due to the extremely small scale of the system, they cannot be measured independently and modeling based on the optical measurements discussed herein is required. Indeed, we find that this microscopic system is extremely complicated and sensitive.

There are two interfacial effects that can cause an "effective pressure difference" at the liquid-vapor interface: capillarity, $\sigma_{lv}K$, which is the product of surface tension and curvature, and disjoining pressure, Π, which models the integral thin film thickness effect of the liquid-solid and liquid-liquid intermolecular forces as an effective pressure. One of the significant effects of the disjoining pressure is that the vapor pressure of an adsorbed completely wetting liquid film is reduced by interfacial forces and therefore, a superheated adsorbed liquid film can exist in (vapor pressure) equilibrium with a bulk liquid at a lower temperature. The effects of temperature and shape can thereby be related in the contact line region. Finite contact angle systems can also be evaluated. Experimentally, we will emphasize spreading (zero contact angle) fluids and will use the following sign convention.

$$P_l - P_v = -\sigma_{lv}K - \Pi \qquad (2)$$

$$\Pi = -\frac{B}{\delta^n} = -\frac{\bar{A}}{\delta^3} \quad , \quad K = \delta'' / [\,1 + (\delta')^2\,]^{3/2} \qquad (3)$$

Equation (2) is the augmented Young-Laplace equation. $\bar{A}$ is the modified Hamaker constant which characterizes the interfacial conditions (i.e., liquid-liquid cohesion versus liquid-solid adhesion). Although the example approximation, $n = 3$, in Eq. (3) restricts its use to thicknesses $\delta \lesssim 20$ nm, the equations can be easily modified for general and/or other specific cases. On the other hand, this approximation also allows important approximate results to be obtained in the thicker film region.

Fluid flow in a curved thin film is also controlled by the pressure gradient. Using the lubrication approximation while neglecting surface shear stress, the mass flow rate per unit width in a slightly tapered thin liquid film is

$$\Gamma = -\frac{\delta^3}{3\nu}\frac{d}{dx}[P_l + \rho_l g x] \qquad (4)$$

The net mass flux of matter crossing a liquid-vapor interface due to a jump change in interfacial conditions at the interface is:

$$\dot{m} = C_l \left(\frac{M_w}{2\pi R}\right)^{1/2} \left(\frac{P_{lv}}{T_{lv}^{1/2}} - \frac{P_{vx}}{T_v^{1/2}}\right) \qquad (5)$$

Herein, we presume that the net mass flux crossing the interface (e.g., evaporation) results from a small vapor pressure drop across an imaginary plane at the interface in which P_{lv}, is the quasi-equilibrium vapor pressure of

the liquid film at ($T_{l/v}$, K, Π, x) and P_{vx} is the equilibrium vapor pressure of a reference bulk liquid (K = 0, Π = 0, x)at a temperature T_v. Neglecting resistances in the bulk vapor space, P_{vx} and T_v can exist at a short distance from the interface, and a resistance to evaporation at the interface can be defined using Eq. (5). Using $T^{1/2}_{l/v} = T^{1/2}_{v} = T^{1/2}_{i}$, this can be rewritten as

$$\dot{m} = C_l \left(\frac{M}{2\pi R T_i}\right)^{1/2} (P_{l/v} - P_{vx}) \qquad (6)$$

Wayner [1991] used a Kelvin-Clapeyron equation for the variation of equilibrium vapor pressure with temperature, disjoining pressure and gravity for the vapor pressure difference in Eq. (6) to obtain

$$\dot{m} = C_l \left(\frac{M}{2\pi R T_i}\right)^{1/2} \left\{ \frac{P_v M \Delta h_m}{R T_v T_{l/v}} (T_{l/v} - T_v) - \frac{V_l P_v}{R T_{l/v}} (\Pi + \sigma_{l/v} K) + \frac{M g P_v}{R T_v} x \right\} \qquad (7)$$

which can be used, along with information on the temperature and shape, to calculate the interfacial mass flux. Equations (1,2,4,& 7) define the one component system with phase change while neglecting surface tension gradients. The ISE and IAI were developed to experimentally evaluate this small system.

3 THEORY FOR THE ISE EXPERIMENTS: AN ISOTHERMAL THIN DRAINING FILM, $\dot{m} = 0$

The experimental results presented below demonstrate that the curvature effect is relatively small in various regions of the isothermal draining film. We analyze these regions first. Neglecting all higher order derivatives of δ with respect to position for the case $\dot{m} = 0$, Eqs. (1, 2, &4) give

$$\frac{\partial \delta}{\partial t} - \left\{ \frac{\rho g \delta^2}{\mu} + \frac{\bar{A}}{\mu \delta^2} \frac{\partial \delta}{\partial x} \right\} \frac{\partial \delta}{\partial x} = 0 \qquad (8)$$

3.1 Equilibrium Adsorbed Thin Film Region

Using Eq.(7) with $\Delta T = 0$ and $\dot{m} = 0$ gives Eq.(9) for the equilibrium film remaining above a drained fluid.

$$\Pi + \sigma K = \rho_l g x \qquad (9)$$

Using Eqs. (3&9) with K = 0 gives Eq. (10) which can be used to obtain the modified Hamaker constant from the *in situ* measurement of the equilibrium film thickness at a particular height above the pool where K = 0.

$$\bar{A} = -\rho_l g x \delta^3 \qquad (10)$$

Since $\bar{A}$ represents the liquid-solid interfacial properties for the experiment based on an *in situ* measurement, the interfacial conditions are accurately known for the experiments.

3.2 Hydrodynamic Region with Low Vapor Pressure where K is Negligible

We use the following similarity variable in Eq. (8) since both "x" and "t" are effectively infinite in extent.

$$\omega = \frac{x_o - x}{t} \qquad (11)$$

Therefore the differential equation for the region where Π is also negligible becomes:

$$\left(\frac{x - x_o}{t^2}\right)\frac{d\delta}{d\omega} + \left(\frac{\rho g \delta^2}{\mu}\right)\left(\frac{1}{t}\right)\frac{d\delta}{d\omega} = \qquad (12)$$

Removing the derivative and solving for the film thickness, δ, gives:

$$\delta = \sqrt{\frac{\mu}{\rho g}\,\omega} \qquad (13)$$

which is the classical result for draining liquid films where Π and K are negligible. Comparison with experimental gives the region where these conditions apply.

4. THEORY FOR THE IAI EXPERIMENTS: A STEADY STATE EVAPORATING MENISCUS

In practice the temperature $T_{l/v}$ is an experimental unknown. Following DasGupta et al. [1993], the one dimensional heat conduction heat transfer solution for the film can be used to eliminate $T_{l/v}$ in favor of T_S in Eq. (6).

$$\dot{m} = \frac{1}{1 + \frac{a \Delta h_m}{k}\delta} \left[a (T_S - T_v) + b (P_{l/v} - P_{vx}) \right] \qquad (14)$$

Where k is the thermal conductivity of the liquid, Δh_m is the enthalpy of vaporization per unit mass, and the coefficients, a and b, are defined as

$$a = C_l \left(\frac{M}{2\pi R T_{l/v}}\right)^{1/2} \left(\frac{P_v M \Delta h_m}{R T_v T_{l/v}}\right),$$

$$b = C_l \left(\frac{M}{2\pi R T_{l/v}}\right)^{1/2} \left(\frac{V_l P_v}{R T_{l/v}}\right) \qquad (15)$$

If the temperature differences are small compared to the absolute temperature, the known substrate temperature, T_S, may be substituted for the unknown $T_{l/v}$ in Eq. (15) to calculate the coefficients "a" and "b". C_l is the accommodation coefficient taken to be 2.0, M is the molecular weight, P_{vx} is the vapor pressure at temperature T_v, V_l is the molar volume of the liquid. According to Eq. (14) evaporation is promoted by superheat and hindered by low liquid film pressure.

This equation clearly demonstrates the direct effect of film thickness and intermolecular forces on the evaporation rate. This model implies that the vapor and solid phases do not present significant resistances to evaporation.

At steady state, the local evaporation rate is linked to the flow rate in the film through a material balance:

$$\frac{d\Gamma}{dx} = -\dot{m} \qquad (16)$$

The boundary conditions are obtained from the consideration that no evaporation can take place from the flat adsorbed film ($\delta=\delta_0$, a constant, as $x \rightarrow \infty$) and hence the pressure gradient in that portion of the film must be equal to zero.

As $x \rightarrow \infty$: $\delta \rightarrow \delta_0$; $(P_l - P_v) = -\frac{a}{b}\Delta T$ where

$$\Delta T = T_s - T_v \qquad (17)$$

5 NUMERICAL SOLUTION TO ANALYZE THE STEADY STATE IAI DATA

As described by DasGupta et al. [1993], the governing equations are non-dimensionalized to obtain

$$\phi = -\frac{1}{\eta^3} - \varepsilon\frac{d^2\eta}{d\xi^2} \qquad (18)$$

$$\frac{1}{3}\frac{d}{d\xi}\left(\eta^3\frac{d\phi}{d\xi}\right) = \frac{1}{1+\kappa\eta}(1+\phi) \qquad (19)$$

Where ξ is the dimensionless position, defined as

$\xi = x/l$ where

$$l = \sqrt{\frac{-\bar{A}}{va\Delta T}}, \quad \bar{A} < 0 \qquad (20)$$

The dimensionless thickness is $\eta = \delta/\delta_0$. ϕ is the dimensionless pressure, defined as,

$$\phi = (P_l - P_v)/\Pi_0, \quad \Pi_0 = \frac{a}{b}\Delta T \qquad (21)$$

The dimensionless groups κ and ε are

$$\kappa = (a\Delta h_m\delta_0/k) \; ; \; \varepsilon = (\sigma\delta_0 bv/-\bar{A}) \qquad (22)$$

The parameter κ is a measure of the importance of the resistance of the film to thermal conduction. The parameter ε is a measure of the importance of capillary pressure effects relative to disjoining pressure effects. These equations demonstrate the importance of both the Hamaker constant and the surface tension. The experimental data on the film thickness profile obtained using the IAI can be fitted with Eq. (19) to obtain κ and ε along with details on $\dot{m}$, P_l, ΔT and $\bar{A}$.

6 MICROSCOPIC IMAGE PROCESSING SYSTEMS TO MEASURE $\delta(x,t)$

We have found that the non uniform film thickness profile can be measured efficiently using a video camera, a microscope, and an image processing system to record the intensity pattern in the reflected light from the film. When non polarized light is reflected from a thin non adsorbing film on a reflecting substrate, interference occurs when the reflected light from the two interfaces of the film recombine. For example, if the relative refractive indices are $n_v < n_F < n_s$, the relevant equation for the film thickness associated with the minima for monochromatic light is

$$\delta = \frac{(2L+1)\lambda}{4\, n_F \cos\phi_l}, \qquad L = 0, 1, 2, 3..... \qquad (23)$$

In which λ is the wavelength of the light and n_F is the refractive index of the liquid film. The thickness profile of the thin film between the minima can also be obtained using the variation of the intensity of the reflected light with film thickness. Since the sensitivity of the reflected light decreases substantially for extremely thin films in the first cycle, we find it advantageous to use ellipsometry for extremely thin films.

Ellipsometry, which can be used to measure film thicknesses down to the order of a monolayer, is concerned with the measurement of changes in the state of polarization of light upon reflection from a surface. Since ellipsometry is a cyclic phenomena, an "interference-like" fringe pattern is also observed. Combined with microscopy and image processing, ellipsometry is also an efficient thickness measuring technique. Although ellipsometry is a more powerful technique, it is much more complicated. The relative phase, Δ, and relative amplitude, Ψ, of the two orthogonal electric field components of the polarized light can be determined from the measured angles of the polarizer, P, the analyzer, A, and the compensator, C, using the standard equation for ellipsometry.

The values of Ψ and Δ can then be used to calculate the refractive index of the substrate or the film thickness and film refractive index. Due to multiple reflections of light at the film-vapor and the substrate-film interfaces, the measured values of Ψ and Δ exhibit an interference effect. In other words, Ψ and Δ are cyclic functions of the film thickness governed by

$$\delta = \lambda/2\,[n_F^2 - n_m^2\,\mathrm{Sin}^2(\Phi_l)]^{0.5} \qquad (24)$$

where n_m is the refractive index of the medium and Φ_l is the angle of incidence. Therefore, when the measured thin film is non uniform, rotating the polarizer and analyzer can only partly extinguish the finite beam of polarized light reflected from the surface. The image appears as a set of destructive fringes representing various film thicknesses. ISE is based on this principle.

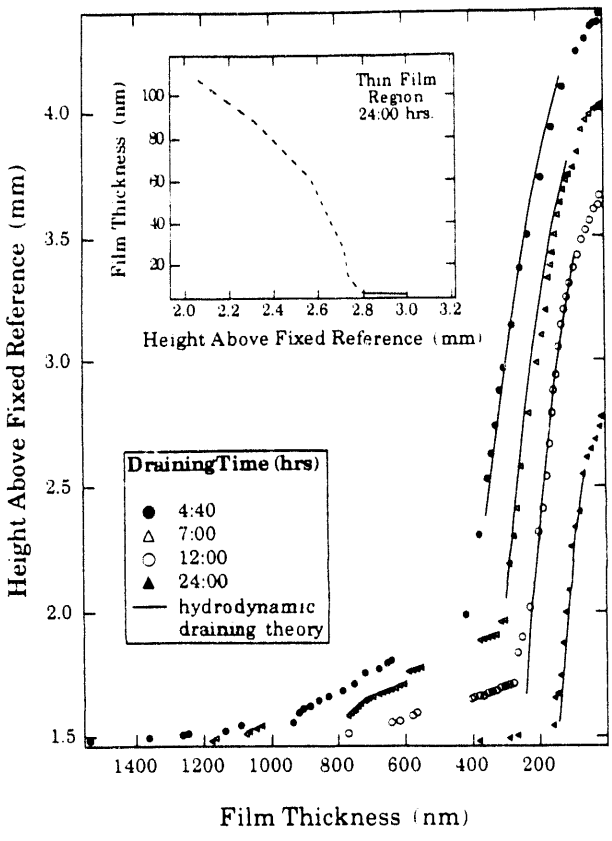

Figure 3 Data on draining thin film of FC-70 on silicon substrate obtained using ISE.

We have developed image processing systems based on both ellipsometry and interferometry. Due to lack of space, the details beyond those given of the design and operation of the image analyzing interferometer, IAI, are given elsewhere in DasGupta et al. [1993] and of the image scanning ellipsometer, ISE, in Liu et al. [1993]

7 EXPERIMENTAL DATA: ISE

Three examples of the measured thickness profiles for FC-70 draining on a vertical plate at t= 4, 12, & 24 hrs. are presented in Fig. 3. We note that, since the thickness scale is different from the height scale by three orders of magnitude , the apparent slopes are misleading. This figure clearly shows that the isothermal draining profiles have at least four distinct regions:

a) The adsorbed thin film region where the modified Hamaker constant, $\bar{A}$, which characterizes the interfacial conditions, can be obtained using Eq. (10). The scale of a portion of this region is expanded in the insert for t = 24 hrs. We find that the thickness of the equilibrium thin film left after drainage is measured in the region x > 3 mm when t = 24 hrs. The thin film with

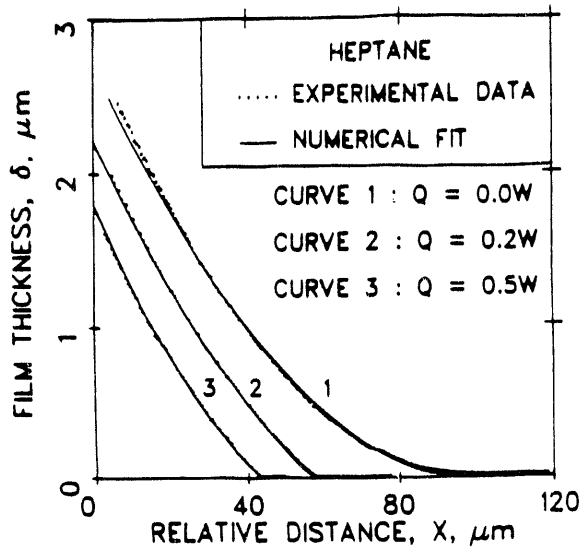

Figure 4. Experimental data obtained using IAI and numerical fit with Eq. (23): Curve 1: Q = 0.0 W, δ_o = 15 ± 0.4 nm, $\kappa = 6.48 \times 10^{-2}$, $\varepsilon = 2.5$; Curve 2: Q = 0.2 W, δ_o = 6.2 ± 0.4 nm, $\kappa = 2.67 \times 10^{-2}$, $\varepsilon = 1.13$; Curve 3: Q = 0.5 W, δ_o = 5.6 ± 0.4 nm, $\kappa = 2.44 \times 10^{-2}$, $\varepsilon = 1.05$;

a very small slope extends for a long distance above the pool. For this system, using δ_o = 5.92 nm at x = 10.2 mm for t > 50 hrs., we find that $\bar{A} = -4 \times 10^{-23}$ J. This characterizes the interfacial conditions.

b) The hydrodynamic draining region which is compared with hydrodynamic draining theory, Eq.(13), in the figure.

c) The transition region between regions (a & b). One of the major advantages of ISE relative to IAI is that we can obtain the details of the dynamic profile in the transition region below a thickness of 100 nm where the influence of the disjoining pressure becomes important.

d) The transition region between the top of the draining classical meniscus and the hydrodynamic draining region where curvature is important. Although the magnification was insufficient with the current design to obtain the curvature in this region at equilibrium, this measurement is achievable. The theoretical height of the equilibrium FC-70 intrinsic meniscus based on only capillarity is 1.38 mm. This was asymptotically attained in the experiments after approximately 50 hours.

We believe that these initial isothermal results demonstrate that the ISE is a convenient and accurate technique to study both isothermal and non isothermal dynamic systems.

8. EXPERIMENTAL DATA: IAI

We have also found that the IAI is an effective technique to study transport processes in thin films.

Examples of the measured thickness profiles fitted with Eq. (19) are presented in Fig. 4. The adsorbed film thicknesses in the flat region (which are not discernible in the figure) were δ_0 = 15 nm for the zero power input case (Q=0, δ_0 = 6.2 nm for Q=0.2W, and δ_0 = 5.6 nm for Q=0.5W. This figure clearly shows that the isothermal profile was more spread out and demonstrates the ability of the IAI to measure the effect of heat transfer on the film profile.

The following procedures were used to obtain additional information concerning the evaporating meniscus from the data. Values of κ and ε are obtained from the measured values of δ_0 and $T_S \approx T_{lv}$ and the numerical fit of the data with Eq.(19). Knowing δ_0 and ε, $\bar{A}$ can be obtained using Eq (22). Knowing δ_0 and $\bar{A}$, ΔT can be obtained using Eq. (21). The maximum heat flux based on kinetic theory for a superheat of ΔT can be obtained using $\dot{m}^{id} = a\,\Delta T$. The results of these calculations for the data presented in Fig. 4 are given in Table (1). Additional results concerning these calculations are given in DasGupta et al. [1993].

Although the fluids are different, it is useful to compare the values of $\bar{A}$ obtained using the ISE with those obtained using the IAI. The substrates were the same. We find that the value obtained using ISE for FC-70 on silicon ($\bar{A} = -4 \times 10^{-23}$ J) is smaller than that obtained using the IAI for heptane on silicon (-1.27×10^{-22} J). This is expected since the surface tension of FC-70 is less than that of heptane.

9. CONCLUSIONS

1. The film thickness profiles of transient or steady state, thin, liquid films can be efficiently and accurately measured using ISE. Whereas, the film thickness profiles of steady state, thin, liquid films can be efficiently and accurately measured using IAI.

2. The thickness profile can be used to evaluate transport processes in thin liquid films.

3. The ISE and IAI are efficient and accurate microscopic image processing techniques to study the intricate details of heat and mass transfer in thin liquid films and to characterize the interfacial conditions *in situ*.

ACKNOWLEDGMENTS

This material is based on work supported by the Department of Energy under Grant #DE-FG02-89ER14045.A000. Any opinions, findings, and conclusions or recommendations expressed in this publication are those of the authors and do not necessarily reflect the view of the DOE. The experimental results have been accepted for publication in Applied Optics.

REFERENCES

Brown, J.R., Chang, W. S., Hallinan, K. P., & Chebaro, H.C. 1993, Heat Transfer from Stable, Evaporating Thin Films in the Neighborhood of a Contact Line, ASME 93-HT-4, National Heat Transfer Conf., Atlanta, GA.

DasGupta,S. ,Schonberg, J. and Wayner, Jr., P. C. 1993, Investigation of an Evaporating Extended Meniscus Based on the Augmented Young-Laplace Equation, J. of Heat Transfer, Vol. 115, 201-208.

Khrustalev, D., and Faghri, A., 1993, Thermal Analysis of a Micro Heat Pipe, Proceedings of 1993 National Heat Transfer Conference, Aug 8-11, Atlanta, Georgia.

Liu, A.H., Wayner, P.C.,Jr., and Plawsky, J.L., 1993, Image Scanning Ellipsometry for Measuring Non-uniform Film Thickness Profiles, To be published in Applied Optics Vol. 32 (probably Dec.).

Swanson, L. W., and Peterson, G. P., 1993, The Interfacial Thermodynamics of the Capillary Structures in Micro Heat Pipes, in Heat Transfer on the Microscale-1993, ed. F.M. Gerner & K.S. Udell, pp. 45-51, HTD-Vol. 253, ASME, National Heat Transfer Conference, Atlanta, Georgia.

Wayner, Jr., P.C. 1991, The Effect of Interfacial Mass Transport on Flow in Thin Liquid Films, Colloids and Surfaces, 52, 71-84 .

Wu, D. and Peterson, G. P., 1991, "Investigation of the Transient Characteristics of a Micro Heat Pipe", J. Thermophysics, vol. 5, pp. 129-134.

Xu, X. and Carey, V. P., 1990, "Evaporation from a Micro-Grooved Surface- An Approximate Heat Transfer Model and its Comparison with Experimental Data," J. Thermophysics, vol. 4, pp. 512-520.

TABLE 1. Characteristics of the Evaporating Heptane Film

Power Input (W)	δ_0 (nm)	ε	$-\bar{A}$ (Joules)	ΔT (°K)	$\dot{m}^{id}$ (kg/m^2•sec)	q^{id} (W/m^2	T_S (°K)
0.0	15	2.50	1.27×10^{-22}	4.5×10^{-5}	6.83×10^{-5}	2.48×10	298.2
0.2	6.2	1.13	1.15×10^{-22}	5.79×10^{-4}	8.76×10^{-4}	3.18×10^{2}	299.9
0.5	5.6	1.05	1.14×10^{-22}	7.60×10^{-4}	1.15×10^{-3}	4.17×10^{2}	302.5

DATE

FILMED

7/7/94

END